Multi-scale modelling of DP590 steel

C. Nikhare, A. Asgari, M. Weiss and P D. Hodgson

Institute for Technology Research & Innovation,
Deakin University, Waurn Ponds 3217, Australia

Abstract

Dual Phase (DP) steel one of the Advanced High Strength Steels (AHSS) has a two phase microstructure where soft and hard phase acts together to offer a high strength composite effect. The high strength, however, must be balanced with ductility so that complex parts and designs can be manufactured from AHSS sheets. However, during forming certain grades of DP steel a sudden crack can occur without any intimation of necking. Thus, due to this abnormal forming behaviour, is difficult to accurately predict because most classical modelling approaches are not designed for such micro-structurally heterogeneous materials. These modelling approaches are generally based on an average representation of the material behaviour in a continuum mechanics formulation. This works for materials that are homogenous, or at least could be assumed to be homogenous at scales lower than the naked eye can see. However, for a material like AHSS, the microstructure plays a significant role in dictating the mechanical behaviour at the macro-scale. This paper studies the multi-scale modelling of DP590 steel. It is found that the sufficient accuracy can be achieved from multi-scale modelling while comparing with the experiments.

1. Introduction

ULSAB (Ultra Light Steel Auto Body) [1] has defined steels with an ultimate tensile strength greater than 700MPa as AHSS. They are generally multiphase steels that contain martensite, bainite and/or retained austenite in quantities sufficient to produce unique mechanical properties. AHSS generally exhibit an excellent combination of high strength and high formability resulting primarily from their high strain hardening capabilities [2-6]. However the material behaviour of AHSS is still not fully understood, and in sheet metal forming AHSS can show high and unpredictable spring-back as well as unpredictable and sudden failure, which is limiting their usage in some applications [7, 8].

In stamping of mild and conventional high strength steel, the typical failure mode is localized necking, resulting in splitting. This type of failure can be related to critical levels of strain in a part [9]. Previous studies performed on Dual Phase (DP) steels have shown that the failure behaviour can be accurately described using FLD curves in cases where localised necking occurs [10-12]. However, in commercial stamping operations involving pronounced bending deformation, fractures have been observed that do not resemble localized necking. In these cases it was not possible to estimate the initiation of fracture using FLD curves [8, 13]. To be able to estimate the initiation of fracture for multiphase steels the necking and fracture behaviour of AHSS for different deformation modes needs to be studied.Previous work has shown that the necking and fracture of steel is significantly influenced by the microstructure. While for conventional steel the necking and fracture properties are generally accurately represented by the mechanical properties obtained from the tensile test, for AHSS divergences have been observed between the forming behaviour indicated by the tensile test and the actual material behaviour in sheet metal forming.

It was further found that the effect of microstructure on the forming behaviour of AHSS depends on the forming path [14, 15]. This finding is especially important in finite element modelling since it suggests that the material behaviour of AHSS can be sufficiently represented by a simple material modelbased on tensile data for some forming applications while, depending on the forming path, for other forming applications more sophisticated material models based on the microstructure are required.

In this study the thinning behaviour of DP steel was studied. The erichsen stretch forming test was performed experimentally. The forming behaviour during stretch forming of this material was simulated by continuum FEA. Further the multi-scale modelling approach based on microstructure is introduced. By comparison with the experimental results the accuracies of the both modelling predictions were analysed.

2. Material and Methodology

2.1 Material

The steel type investigated in this study is DP590. The measured thickness and chemical composition, as given by the supplier, are shown in Table 1

Table 1 Chemical composition range of DP steel

Desig-nation	Thickn-ess(mm)	Chemical Composition, wt %				
		C	Mn	Si	Al	Nb
DP	1.97	0.069	1.410	1.040	0.022	0.011

2.2 Methodology

The thinning behaviour in biaxial strain of the DP590 steel was determined by stretch forming tests. The thinning of this material during forming was measured using optical microscopy [16]. To investigate whether the thinning behaviour of the steel can be accurately predicted by a simple continuum model FEA approach, the stretch forming test was simulated using FEA and compared to the experimental results. Furthermore the multi-scale modelling approach was introduced to predict the same and compared with experiment and continuum model.

2.2.1 Tensile test

The tensile tests were performed as recommended in Australian standard AS 1391-1991 on specimens and the test procedure is explained in [16].

2.2.2 Erichsen stretch forming

Stretch forming test was performed using the Erichsen sheet metal tester and the tooling shown in Figure 1. For the test, a sandwich construction of oil together with polymer foil was used for lubrication. The punch speed and blank-holding force applied were 0.1 m/min and 230 kN, respectively. The test was stopped at a final punch stroke 22 mm to measure the thickness distribution [16].

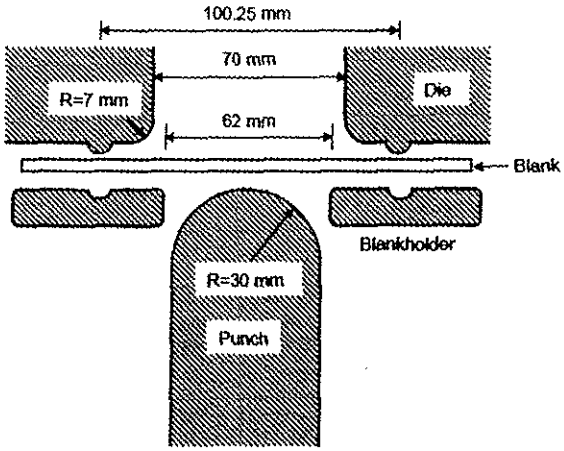

Figure 1 Experimental set-up of Erichsen stretch forming

2.2.3 Numerical Modelling

The stretch forming tests was investigated using ABAQUS/Explicit 6.5-1 with a three-dimensional model approach. The tooling was given as rigid surfaces, while S4R shell elements (Four node, reduced integration) were used to mesh the blank. Only a quarter of the blank was used in the model because of the axis-symmetry of both tests. The average sheet thickness measured experimentally for the steel (see Table1) was detailed in the model and the true stress-strain data, determined in the tensile test, was applied to define the material properties of the particular steel type using isotropic hardening. Since the fitted power law did not correlate well with the initial region of metal plastic definition (see results and discussion section), the material input used to represent the material behaviour of the three steel grades was a combination of experimental test data (initial part of the hardening curve) and material data extrapolated of the fitted power laws (later stages of the hardening curve) [16].

Generally, the same process parameters as present in the experimental test were applied in the model. For the simulation of the stretch forming process the flange region of the specimen was neglected and the outside edge was fixed in the boundary conditions. This assumes a perfect clamping and no movement of the specimen between the blankholder and the die surface. Because of the high lubrication used in the stretch forming test, zero friction was assumed in the FEA approach between the blank and the punch.

2.2.4 Multi-scale Modelling

The as-received microstructure of DP590 steel was considered to generate the micrograph (Figure 2) of 150X200 pixels size with the help of OOF2 software. The micrograph divides in the ferrite (gray) and martensite (dark) mesh. The micrographs were further imported in Abaqus CAE and analysed as 2D plane strain elements (CPE8R: An 8-node biquadratic plane strain quadrilateral, reduced integration). The ferrite and martensite material properties were fed for ferrite and martensite region of microstructure. The ferrite was assumed as the softest material (K=300MPa and n=0.13) and further from the DP tensile curve; the martensite curve was plotted (as the average of ferrite and martensite curve is DP curve). The periodic boundary conditions were applied in the model. The assumed deformation gradient was then applied to deform the microstructure to generate the DP flow curve through microstructure.

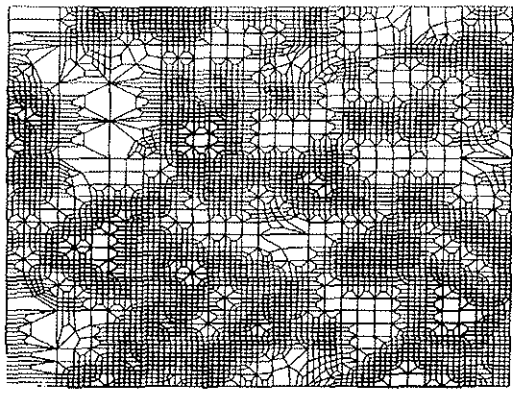

Figure 2 DP Micrograph for micro-scale modelling

3 Results and Discussion

3.1 Tensile test

The true stress-strain curve determined in the tensile test is shown in Figure 3. The stress strain curve was fitted using a power law,

It is clear that for the material, the fitted power law does not give a good representation of near yield behaviour. This is, because a tensile region above 10% strain was used to determine the hardening exponent.

The mechanical property of the DP steel is summarized in Table 2.

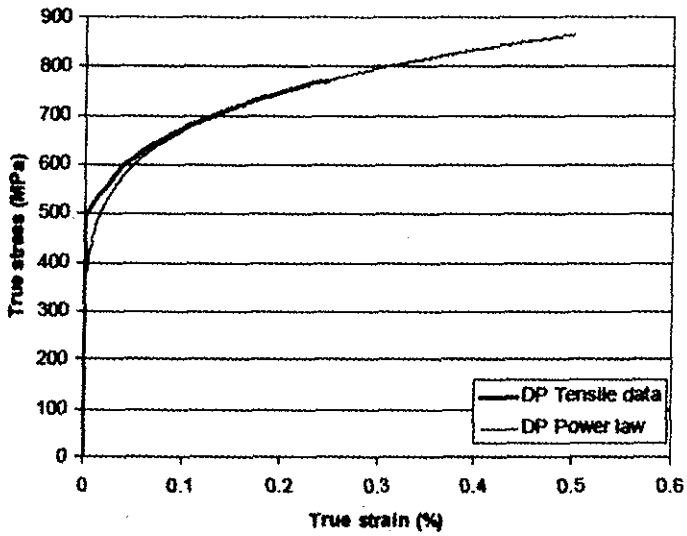

Figure 3 Experiment true stress-strain curves fitted with the power law for DP steel

Table 2 Mechanical properties of DP steel

Designation	Mechanical Properties				
	Yield strength (MPa)	Tensile strength (MPa)	Elongation, %	K (MPa)	n
DP	491	771	30	965	0.1585

3.2 Stretch forming test

To measure the thickness distribution of the sample, from stretch formed cup, a strip was cut out of the dome section (figure 4) and prepared as explained in [16]. The thickness distribution over the dome surface for the region A is shown in Figure 5. The thickness at the top centre is 1.116mm which is around 43.35% strain.

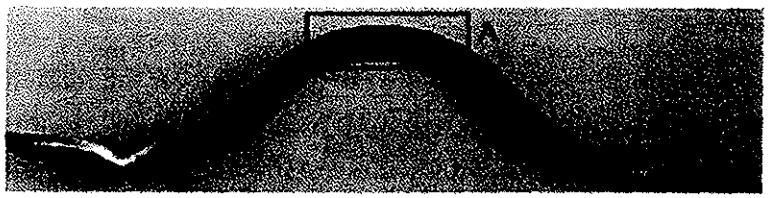

Figure 4 Cut strip in stretch forming for thickness measurement

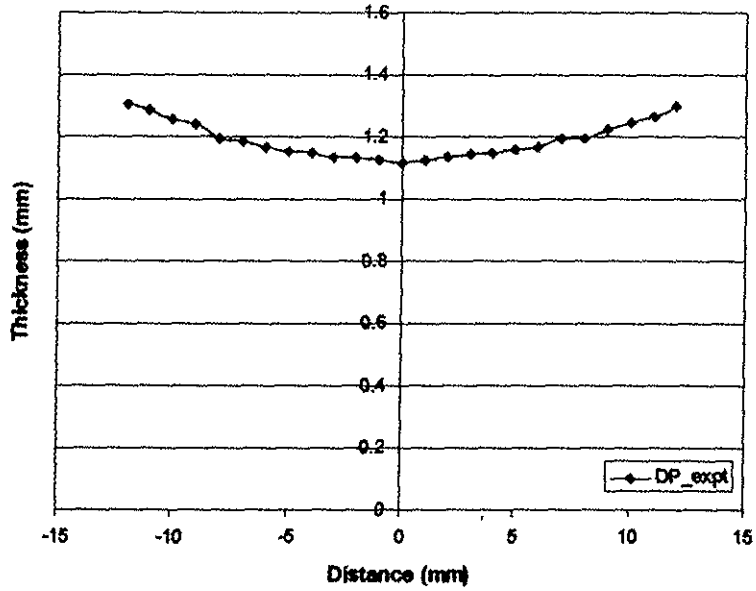

Figure 5 Experimental thickness distribution measured over the dome

3.3 Continuum FEA model

Figure 7 shows the comparison of continuum FEA model predicted thickness with the experiments. The continuum FEA model shows the inaccuracy in predicting the thickness distribution. Thus more a sophisticated material model is needed to predict the result accurately.

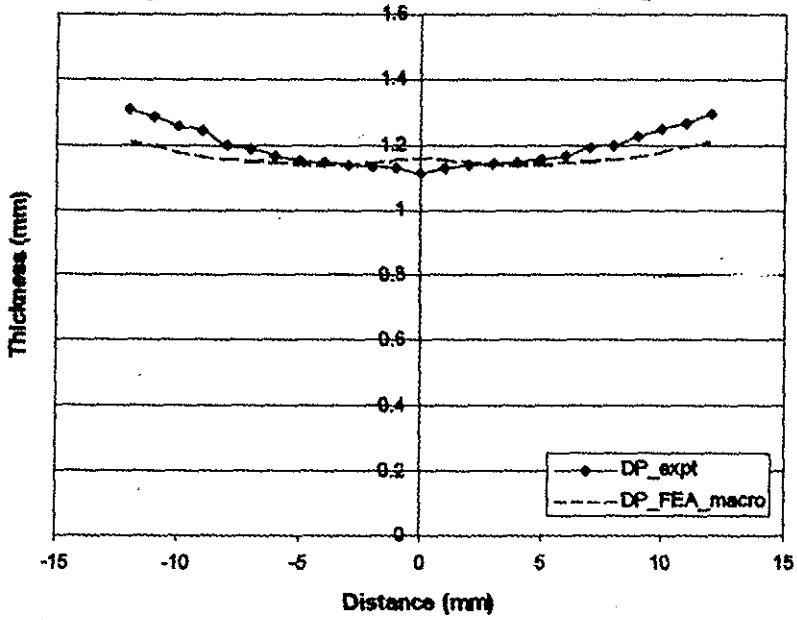

Figure 7 Experimental and Continuum model thickness distribution measured over the dome

3.4 Multi-scale model

Based on assumed ferrite flow curve and the DP tensile curve, the martensite flow curve is calculated and fitted with the power law (K=1650MPa and n=0.17) and is shown in Figure 8. The ferrite and martensite flow curve then fed to simulate the DP micrograph. Figure 9 shows the deform micrograph.

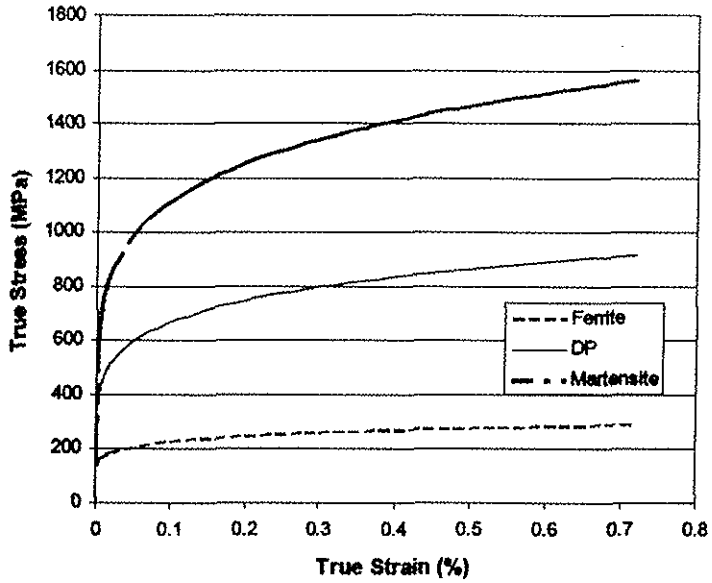

Figure 8 Flow curves for Ferrite, Martensite and DP steel

Figure 9 Deform micrograph

The stress-strain data for the whole micrograph is calculated by performing the volume average per increment. The flow curve resulted from this micrograph is the DP curve based on microstructure and is called as DPmicro in this paper (Figure 10). The DPmicro curve is fitted with the power law (K=930MPa and n=0.17) and shows that the hardening is bit lower than the actual DP curve from tensile test (Figure 10).

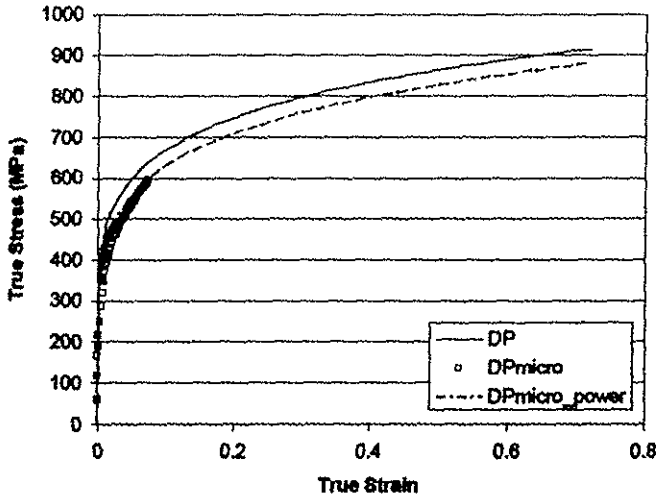

Figure 10 Flow curves of DP and DP micro with fitted power law

Figure 11 shows the comparison of thickness distribution between multi-scale model, continuum model and the experiment. The thickness distribution through multi-scale model shows more thinning than the continuum model and is closer to the experiment results.

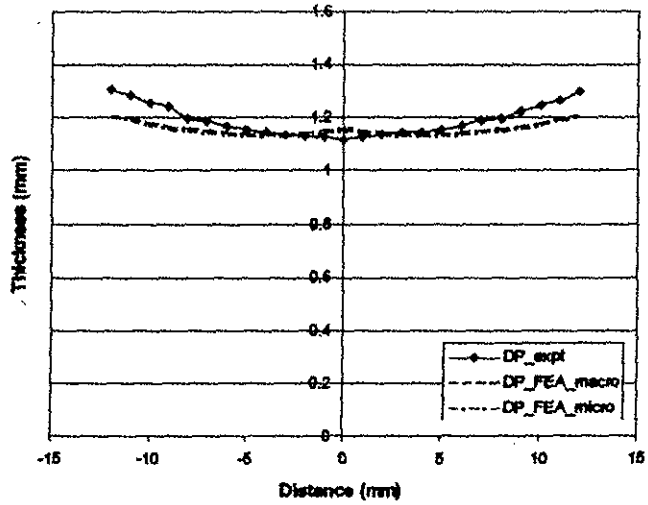

Figure 11 Experimental, Continuum model and Multi-scale model thickness distribution measured over the dome

Conclusion

The thinning behaviour of the DP steel was determined during stretch forming test. The continuum FEA model approach was applied to predict the thinning but is failed to represent the same thinning behaviour during the stretch forming process. This has been related to differences in microstructure. This indicates that a more sophisticated material model is necessary to represent the forming behaviour of advanced high strength steels in stretch forming. Thus the multi-scale modelling approach was introduced and comparison shows that the sufficient accuracy can be achieved.

Acknowledgement

This research was supported by Deakin University and ARNAM. Professor Peter Hodgson acknowledges the support at the ARC through his Federation Fellowship.

References

1. **International Iron and Steel Institute:** Project reports on UltraLight Steel Auto Body-Advanced Vehicle concepts (ULSAB-AVC), www.worldautosteel.org.
2. **Horvath, C. D. (2004):** The Future Revolution in Automotive High Strength Steel Usage. 2004, www.autosteel.org/pdfs/gdis_2004_horvath.pdf.
3. **Satorres, A. (2005):** Bending simulation of high strength steel by finite elements. Master's Thesis, University of Oulu.
4. **Bhadeshia, H. K. D. H. (2002):** TRIP-Assisted steels? ISIJ International, vol 42(9), pp. 1059-1060.
5. **Fekete, J. R. (2005):** Manufacturing Challenges in Stamping and Fabrication of Components From Advanced High Strength Steel. Int. Symp. On Niobium Microalloyed Sheet Steel for Automotive Applications, The Minerals, Metals and Material Society (TMS), pp. 1.7-115.
6. **Horvath, C. D.; Fekete, J. R. (2004):** Opportunities and Challenges for Increased Usage of Advanced High Strength Steels in Automotive Applications. Proc. Int. Symp. On Advanced High Strength Steels for Automotive Applications, Association for Iron & Steel Technology.
7. **Wagoner, R. H.; Smith, G. R. (2006):** Report Draft Advanced High Strength Steel Workshop. The Ohio State University.
8. **Fekete, J. R. (2007):** Current challenges in Implementing Advanced High Strength Steels. International Conference on Microalloyed Steels: Processing, Microstructure, Properties and Peformance, pp. 1-9.
9. **Hosford, W. F.; Caddell, R. M. (1993):** Forming Limits. Metal Forming- Mechanics and Metallurgy, Second Edition, Prentice Hall, pp. 309-325.
10. **Konieczny, A. A. (2001):** On Formability Assessment of Automotive Dual Phase Steel. International Body Engineering Conference (IBEC), SAE Technical Paper # 2001-01-3106.
11. **Sriram, S.; Yan, B.; Huang, M. (2004):** Characterization of Press Formability of Advanced High Strength Steels Using Laboratory Tests. SAE Technical Paper No. 2004-01-0506.
12. **Shi, M. F.; Gelisse, S. (year):** Issue on the AHSS forming limit Determination.
13. **International Iron and Steel Institute (2005):** ADVANCED HIGH STRENGTH STEEL (AHSS) APPLICATION GUIDELINES. Online at www.worldautosteel.org
14. **Yamazaki, Y. (2003):** Current situation and properties of Ulta-high Strength Steel for automotive use in Japan. La Revue de Metallurgie, pp.779-786.
15. **Hasegawa, K.; Kawamura, K.; Urabe, T.; Hosoya, Y. (2004):** Effects of microstructure on stretch-flange-formability of 980MPa Grade cold-rolled Ul High Strength Steel sheets. ISIJ International, vol. 44, no. 3, pp. 603-609.
16. **Nikhare, C.; Marcondes, P. V.; Weiss, M.; Hodgson, P. D. (2008):** Experimen and numerical evaluation of forming and fracture behaviour of high strength st New Developments on Metallurgy and Applications of High Strength Steels, Bue Aires.